



# Synergistic effect of catalytic co-pyrolysis of cellulose and polyethylene over HZSM-5

Yuying Zhao<sup>1</sup> · Xiaoxiao Yang<sup>1</sup> · Zewu Fu<sup>1</sup> · Rui Li<sup>1</sup> · Yulong Wu<sup>2,3</sup>

Received: 11 March 2019 / Accepted: 24 July 2019 / Published online: 7 August 2019  
© Akadémiai Kiadó, Budapest, Hungary 2019

## Abstract

This study investigated the synergy in the co-pyrolysis of cellulose and polyethylene (PE) over HZSM-5 and the mechanism of the catalytic co-pyrolysis. PE, cellulose, cellulose/PE, cellulose/PE/HZSM-5 were subjected to thermogravimetric analysis and Py-GC/MS experiments at 650 °C to obtain the distribution of products, respectively. The results of Py-GC/MS experiments showed that the products quality of co-pyrolysis of PE and cellulose is improved over HZSM-5. The mechanism of catalytic co-pyrolysis was mainly the radical reaction and Diels–Alder reaction. The catalytic effect of HZSM-5 was mainly to promote the Diels–Alder reaction to produce more aromatic hydrocarbons. According to the density functional theory, the mechanism of this catalytic co-pyrolysis was verified, and the proposed reaction paths were verified to make the co-pyrolysis process more clear.

**Keywords** Cellulose · Polyethylene · Py-GC/MS · Mechanism · Density functional theory

## Introduction

The rapid consumption of fossil fuels and the increase in energy demand have aroused interest in the use of biomass as a renewable energy source. China, a large agricultural and forestry country, is rich in biomass resources, so

biomass is an effective substitute for fossil fuel. Pyrolysis technology is a clean and efficient thermal conversion method that can convert biomass into bio-oil and chemicals [1–5]. However, bio-oil produced by biomass pyrolysis has high oxygen content, low calorific value, high content and viscosity of water and acid, and cannot be used directly [1].

Catalytic pyrolysis of biomass is a promising technology, which can convert lignocellulose into valuable aromatics and olefins [1]. Some volatile intermediate materials (such as anhydrosugar, furan and phenols) further catalytically convert the initial thermal decomposition products of biomass into aromatics and olefins through a series of reactions, including cracking, deoxygenation, oligomerization, and aromatization on zeolite catalysts [1]. The main products such as benzene, toluene, xylenes, and naphthalenes are main petrochemical feedstocks [4, 5].

Although the bio-oil produced by catalytic pyrolysis is significantly improved compared with the bio-oil produced by simple pyrolysis, there are still problems such as excessive coke and tar residue [6]. The addition of a co-reactant rich in carbon and hydrogen can increase the yield and can extend catalyst life by reducing coke formation. Specially, catalytic co-pyrolysis of plastics and biomass has been shown to promote conversion to aromatic hydrocarbons, and also provided a productive treatment of

---

✉ Rui Li  
boxlr@126.com

✉ Yulong Wu  
wulong@tsinghua.edu.cn

Yuying Zhao  
zhaoyuying@bjfu.edu.cn

Xiaoxiao Yang  
13020021531@163.com

Zewu Fu  
930951675@qq.com

<sup>1</sup> MOE Engineering Center of Forestry Biomass Materials and Bioenergy, Beijing Forestry University, Beijing 100083, China

<sup>2</sup> Institute of Nuclear and New Energy Technology, Tsinghua University, Beijing 100084, China

<sup>3</sup> Key Laboratory of Advanced Reactor Engineering and Safety of Ministry of Education, Tsinghua University, Beijing 100084, China

discarded agricultural plastics [4, 5, 7, 8]. The main reason for these problems is due to the lower effective hydrogen/carbon ratio ( $H/C_{\text{eff}}$ ) of the biomass (0–0.3). In 1986, Chen et al. proposed the concept of an effective hydrogen/carbon ratio (Eq. 1) for estimating whether a feedstock can be economically converted into a hydrocarbon chemical [1–5].

$$H/C_{\text{eff}} = \frac{H - 2O}{C} \quad (1)$$

Raw material with a  $H/C_{\text{eff}}$  value of 1–2 can produce petroleum products, while raw materials with a  $H/C_{\text{eff}}$  value lower than 1 produce more coke [4–6, 9–13]. Therefore, it is necessary to add H-rich raw materials to the biomass pyrolysis process to increase  $H/C_{\text{eff}}$ .

Plastic is a cheaper polymer with high  $H/C_{\text{eff}}$ . Such as polyethylene (PE), polypropylene (PP), and so on, its  $H/C_{\text{eff}}$  can reach 2. In addition, plastic resources are abundant, and global plastic production is increasing every year [8]. Polymer waste can take billions of years to degrade naturally, with serious environmental consequences. Secondary reuse is of significant importance both in the management of environmental pollution and in the development of renewable energy [9, 12]. Currently, the methods of treating plastic waste include incineration or landfill disposal. Incineration can produce useful energy, but it also releases toxins. Comparison to incineration, pyrolysis produces fewer toxins due to lack of oxygen. In summary, co-pyrolysis of biomass and plastic is a promising technology, which can convert biomass and waste plastics to liquid fuels and chemicals [1, 9, 12, 14–17].

At present, there have been many studies in co-pyrolysis of biomass and waste plastic. Some researches indicated that no synergistic effect was found in the co-pyrolysis of the biomass and plastic without catalyst [16, 18]. Meanwhile, some researches indicated that the co-pyrolysis of biomass and plastics increased the production of bio-oil and the alcohol content. Studies have shown that catalysts can change the reaction path during pyrolysis and reduce the activation energy of the reaction [1, 2, 4, 19–23]. Some researchers have also inferred the reaction mechanism of catalytic co-pyrolysis of the biomass and plastic from the molecular level [1, 3–5].

However, in the recent studies, an exact catalytic co-pyrolysis reaction mechanism has not yet been given, and the research is still based on preliminary assumption. Therefore, the entire chemical reaction process of catalytic co-pyrolysis is still unclear [3–6, 24–32]. The knowledge is vital in the process of catalytic co-pyrolysis. Because we want to study the advantages of catalytic co-pyrolysis over pure pyrolysis, we must start with the reaction mechanism, clarify the progress of each step, and better explore how to improve the conditions and influencing factors of catalytic

co-pyrolysis, in order to improve the quality of bio-oil further.

By investigating the effect of co-pyrolysis on the product distribution, this research aimed to improve the pyrolysis product distribution and infer the reaction mechanism of co-pyrolysis of cellulose and PE over HZSM-5 based on the analysis of the pyrolysis products and theoretical calculations. The density functional theory (DFT) in Gaussian calculation was used to simulate each reaction path of catalytic co-pyrolysis proposed by our research, and the inferred catalytic co-pyrolysis reaction mechanism was verified.

## Materials and method

### Materials

Microcrystalline cellulose was purchased from Beijing Kebaiao Biotechnology Co., Ltd. Polyethylene (1000 mesh) was purchased from Dongguan Huangjiang Shengbang Plastic Materials Co., Ltd. Carbon, hydrogen, and nitrogen contents of the cellulose and PE were analyzed with an elemental analyzer (CE-440, Exeter Analytical, Inc., North Chelmsford, MA). HZSM-5 was purchased from Yangzhou Zhonghe Petrochemical Research Institute Co., Ltd., with a silicon–aluminum ratio of 30:1. Cellulose and PE were mixed evenly at the ratio of 1:1. Cellulose, PE, and HZSM-5 were mixed evenly at the ratio of 1:1:4. All the raw materials and catalyst were powdered.

### Thermogravimetric experiments

Thermogravimetric analysis (TGA) was performed using a thermal analyzer (TG Instruments SDT-Q600). TGA experiments were conducted on 5 mg samples (individual feedstock and blends) in inert atmosphere ( $N_2$ ), using a ramp rate of  $30\text{ }^\circ\text{C min}^{-1}$ , to the final temperature of  $650\text{ }^\circ\text{C}$ . The flow rate of  $N_2$  was  $50\text{ mL min}^{-1}$ .

### Analytical pyrolyzer coupled with gas chromatograph–mass spectrometer (Py–GC/MS)

Pyrolysis experiments were carried out using the EGA/PY-3030D pyrolyzer (Frontier Laboratories, Japan) equipped with the gas chromatograph–mass spectrometer (QP2010Ultra, Shimadzu, Japan).  $0.5 \pm 2\%$  mg sample [cellulose, PE, their mixture (1:1 in mass), and their mixture over HZSM-5 (1:4 in mass)] was pyrolyzed in the quartz tube in each test. All pyrolysis processes were carried out at  $650\text{ }^\circ\text{C}$ , 30 s with heating rate of  $20\text{ }^\circ\text{C ms}^{-1}$  using a platinum coil probe and quartz sample tubes. GC analyses were performed on a DB-5MS capillary column

(30 m × 0.25 mm × 0.25 μm). The oven was programmed to hold at 40 °C for 5 min and was ramped at 5 °C min<sup>-1</sup> to 180 °C for 5 min and then was ramped at 5 °C min<sup>-1</sup> to 280 °C, after which it was held at this temperature for 5 min. The injector temperature was kept at 280 °C with the injector split ratio set to 80:1, and helium flow rate was maintained at 0.8 mL min<sup>-1</sup>. MS detection was carried out under electron impact (EI) ionization conditions in full scan from 33 to 500 m z<sup>-1</sup> with a threshold at 70 eV, a scan rate of 500 Da s<sup>-1</sup>, and an ion source temperature of 230 °C. All mass spectra were compared to the NIST11 mass spectrum library.

## Calculation method

All calculations were carried out with the Gaussian 09 W suite of programs [31]. The initial model of the reactants, intermediates, and final products involved in the initial reaction of catalytic co-pyrolysis was structurally optimized under B3LYP/6-31G (d) to find the most stable geometry and then search for related reactants in the transition state [32, 33]. For the corresponding product, the transition state has only an imaginary frequency, and the reactants, intermediates, and products have no imaginary frequency. The transition state is followed by the TS method in two directions following the intrinsic reaction coordinate (IRC) analysis to ensure that the transition state is related to the correct reactants and products. Frequency analysis and IRC analysis were performed using the same basis set as the optimization. Single-point energy (SPE) was obtained using the M062X/def2TZVP level, which is more accurate than B3LYP/6-31 G (d) in calculating the energy of organic matter. All calculations were performed at 650 °C.

## Results and discussion

### Elemental composition analysis

The elemental composition of the cellulose and PE samples and the  $H/C_{\text{eff}}$  of them and their mixtures are listed in Table 1. As reported in Table 1, the  $H/C_{\text{eff}}$  of cellulose samples was 0, and the  $H/C_{\text{eff}}$  of PE was 2. Based on the  $H/$

**Table 1** Elemental analysis of the cellulose and PE samples used in this study

Feedstock/%	N%	C%	H%	S%	O%	$H/C_{\text{eff}}$
Cellulose	0.16	44.6	6.6	0	49.1	0
PE	0	85.7	14.3	0	0	2

$C_{\text{eff}}$  of cellulose and PE samples, the  $H/C_{\text{eff}}$  of their mixtures was 1.3. The result suggested that the addition of PE has increased the  $H/C_{\text{eff}}$  of their mixture which proved that PE acted as a hydrogen donor.

### Thermogravimetric (TG) and derivative thermogravimetric (DTG) analysis

The TG (a) and DTG (b) curves of pyrolysis of cellulose, PE, cellulose/PE, cellulose/PE/HZSM-5 are shown in Fig. 1. The main mass loss ranges of cellulose, PE, cellulose/PE, cellulose/PE/HZSM-5 are shown in Table 2. The results in Fig. 1b indicate that the main mass loss range of cellulose is 300–420 °C, the maximum mass loss rate appears at 370 °C, the main mass loss range of PE is 400–530 °C, and the maximum mass loss rate appears at 490 °C. According to the DTG curve, there are two pyrolysis stages of co-pyrolysis of cellulose and PE. The first stage is 270–410 °C, and the maximum mass loss rate appears at 365 °C. The second stage is 440–540 °C, and the maximum mass loss rate appears at 490 °C. It is shown

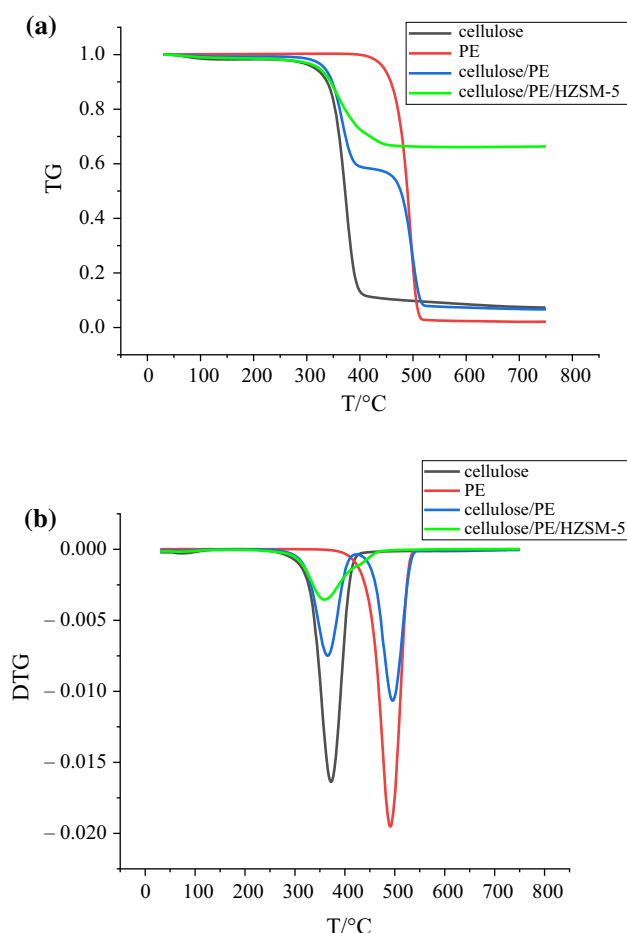


**Fig. 1** a TG and b DTG curves of pyrolysis of cellulose, PE, cellulose/PE, cellulose/PE/HZSM-5

**Table 2** Characteristic pyrolysis parameters of cellulose, PE, cellulose/PE, cellulose/PE/HZSM-5

Feedstock	Decomposition temperature range/°C	Maximum mass loss temperature/°C
Cellulose	300–420	372
PE	400–530	490
Cellulose/PE	270–410 and 440–540	365 and 490
Cellulose/PE/HZSM-5	270–500	360

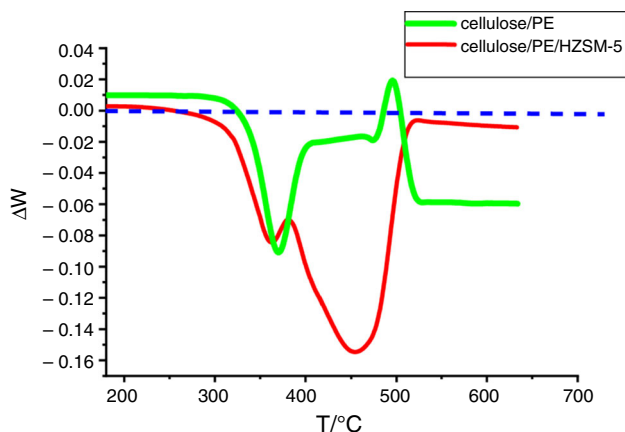
that the cellulose and PE have different temperatures of maximum mass loss rate, and the pure mixture of them has no significant synergism. Notably, for the catalytic co-pyrolysis of mixture over HZSM-5, there is only one pyrolysis stage according to the DTG curve (Fig. 1b), the decomposition range is 270–500 °C, and the maximum decomposing rate appears at 360 °C.

Figure 2 shows the  $\Delta W$  curves of cellulose/PE and cellulose/PE/HZSM-5, and the  $\Delta W$  curve was calculated by Eq. 2.

$$\Delta W = W_{\text{blend}} - (W_1 \times x_1 + W_2 \times x_2 + W_3 \times x_3) \quad (2)$$

Here, the  $W$  in Eq. 2 is the mass during the mass loss, subscript blend is mixture, 1 is cellulose, 2 is PE, 3 is HZSM-5, and the  $x$  is the proportion of the mixture.

As can be seen, when the mixture without HZSM-5, PE inhibits the mass loss of cellulose in the range of 330–400 °C and PE promotes mass loss of cellulose in the range of 480–500 °C. The reason for this phenomenon is that PE coated with cellulose inhibits the escape of volatiles after melting in the range of 330–400 °C. As the temperature rises further, PE cracks and produces olefins which react with free radicals generated by pyrolysis of cellulose to form volatile substances, so that it increases the mass loss rate in the range of 480–500 °C. However, when HZSM-5 was added into the sample, loss of cellulose mass is suppressed throughout the temperature range, and the most inhibited temperature range is 350–500 °C. HZSM-5 promotes the reaction of the products produced by cellulose and olefins; therefore, the free radical reaction

**Fig. 2**  $\Delta W$  curves of cellulose/PE and cellulose/PE/HZSM-5

mentioned earlier is suppressed. Since the reaction products of the latter were more stable than that of the former, the mass loss of sample over with HZSM-5 was less than without HZSM-5. All these results indicate that the co-pyrolysis of cellulose and PE has a significant synergistic reaction after the addition of HZSM-5.

### Pyrolyzer coupled with gas chromatograph–mass spectrometer (Py-GC/MS) analysis

The GC/MS chromatograms of the samples that pyrolyze at 650 °C for 30 s are shown in supplementary materials. According to related studies, NIST11 mass spectrum library, the main identified pyrolysis products of cellulose, PE, and their mixture are shown in Fig. 3a. The main chemical compounds were identified corresponding to different retention time. They were divided into oxygenated, olefins, alkenes, and aromatics groups first. Then, the remaining compounds were divided into the “others” group, and the others are mainly salt compound, amine, etc., such as pentafluoropropionate, ammonium acetate, and propanamine.

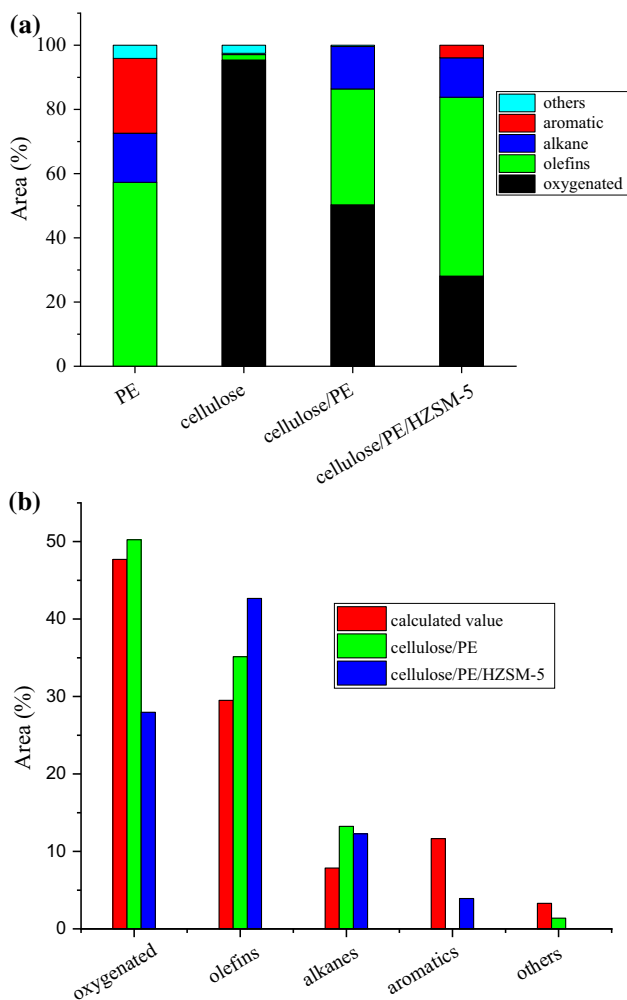
### Pyrolysis of cellulose, PE, and their mixture without catalyst

Figure 3a indicates that oxygenated compounds are the main pyrolysis product of cellulose, and its proportion is high to 95.4% of all the products. Figure 4 shows that the saccharides are major product of oxygenated compounds, which takes up 36.8% of pyrolysis product of cellulose. Besides saccharides, alcohol, ester, ketone, aldehyde, furan, acids also exist in the pyrolysis, which take up 33.83, 14.16, 8.08, 1.41, 1.04, and 0.06%, respectively. As for PE, the main pyrolysis product of PE shown in Fig. 3a is olefins, aromatics, and alkanes, which account for 57.3, 23.3, and 15.3%, respectively. When PE is mixed with cellulose at the ratio of 1:1, the oxygenated chemicals decrease from 95.4 to 50.3%, and the percentage of their mixture is similar to the calculated value.

The calculated value is obtained from Eq. 3.

$$\text{Calculated value} = x_1 \times \text{Cellulose value} + x_2 \times \text{PE value} \quad (3)$$

In Eq. 3, the cellulose value is the yield of pure cellulose, the PE value is also the yield of pure PE [1, 19], and  $x$



**Fig. 3** Distribution of product pyrolysis from **a** PE, cellulose, cellulose/PE, cellulose/PE/HZSM-5 and **b** cellulose/PE, cellulose/PE/HZSM-5, the calculated value of cellulose and PE

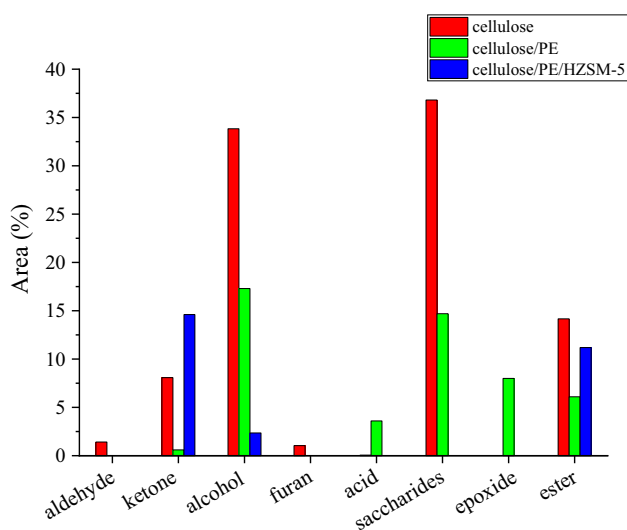


**Fig. 4** A comparison of the types and contents of oxygenates in cellulose, cellulose/PE, cellulose/PE/HZSM-5 pyrolysis products

is the proportion of the sample. The distribution of the product pyrolysis from cellulose/PE, cellulose/PE/HZSM-5, and the calculated value of cellulose and PE is shown in Fig. 3b.

Comparing the contents of the compounds in Fig. 3a, b, the addition of PE has not changed the percentage of products essentially. To some extent, the mixture of cellulose of PE has no obvious effect on the distribution of products as expected [34–41].

From Fig. 3a, we can see the oxygenated chemicals takes up 28.1% of all of the pyrolysis products, and olefins, alkanes, and aromatics account for 55.7, 12.3, and 3.9%, respectively. According to Fig. 3a, comparing with the pyrolysis of the mixture without HZSM-5, the oxygenated compounds of the pyrolysis product over HZSM-5 added are significantly reduced while the olefins is increased. The aromatics appear in the products of the pyrolysis over HZSM-5, when there are almost no aromatics in the pyrolysis products without HZSM-5. The special pore structure and surface acid sites of HZSM-5 may play a crucial role in aromatics formation. This is because HZSM-5 has a two-dimensional pore system, its pore size is comparable to that of benzene molecule, and it has good shape selectivity. In addition, the Lewis and Brønsted sites of HZSM-5 are contained in the micropores, at which deoxygenation and aromatization of cellulose are occurred to form aromatics and olefins [1, 40–46]. Olefins and alkanes derived from PE are also further cracked due to the effects of Lewis and Brønsted sites [3]. Therefore, the synergism between cellulose and PE is obvious when HZSM-5 is added into the sample. The alkanes produced by the pyrolysis of cellulose alone are only 0.4%, the alkanes produced by pyrolysis of their mixture is 13.2% while the alkanes produced by the pyrolysis of PE alone are 15.3%. Figure 3b shows that the calculated values of oxygenates are higher than the experimental values of the mixture over with HZSM-5 and are lower than the mixture over without HZSM-5. Herein, the addition of the HZSM-5 can induce the content of the oxygenates. However, the calculated values of the olefins and the alkanes are lower than the experimental values. On the contrary, the aromatics calculated are lower than the experiment. It is implied that there is no positive effect on the production of aromatics between cellulose and PE without HZSM-5.

A comparison of the kinds and contents of oxygenates in cellulose, cellulose/PE, cellulose/PE/HZSM-5 pyrolysis products is shown in Fig. 4. Among the cellulose pyrolysis products, alcohols and sugars are the main oxygenates. When PE is added, the content of alcohols, acids, and saccharides is reduced, and epoxide and ester compounds are present. After adding HZSM-5, the content of the alcohol is lower, the acids and the saccharides disappear, and the content of the ketone and the esters increases.

## Reaction path and DFT calculation

Many studies have speculated on the reaction mechanism of cellulose and plastic waste. According to previous speculations and the support of these experimental data: Cellulose pyrolysis products are mainly oxygenates, including saccharides, alcohols, ketones, aldehydes, and furans; after the addition of PE, the content of oxygenates is reduced, but the synergistic effect is not particularly strong. After adding HZSM-5, the content of oxygenates is lower than that of cellulose and PE, and esters and ketones are lower. The kinds of the oxygenates increase and aromatics of the oxygenates appear. The reaction mechanism of cellulose and PE over on the catalysis of HZSM-5 was proposed as shown in Fig. 5 [1, 4, 19].

Cleavage, dehydration, and decarboxylation of cellulose mainly produce aldehydes, alcohol, furans, and their derivatives, and the resulting furan, furan derivatives, and acetol react with olefins produced by PE cracking under the action of a catalyst. Among them, the hydroxyl group produced by pyrolysis of pyruvic acetol and the vinyl group produced by PE cracking react with a radical to form vinyl alcohol [1, 40]. It has been suggested in the literature that hydroxyl groups are produced during the pyrolysis of cellulose, but there is no specific indication that the hydroxyl groups react with the vinyl groups produced by PE cleavage to obtain alcohols. This article clearly states that a free radical reaction between a hydroxyl radical and a vinyl group produces an alcohol. Furan and its derivatives react with olefins produced by PE cracking to form aromatic hydrocarbons (benzene, toluene, xylene, etc.), which is known as Diels–Alder reaction and dehydration reactions. This can promote the generation of aromatics. Furthermore, PE-derived hydrocarbons such as alkanes and olefins can provide hydrogen for cellulose-derived oxygenates, which can reduce the amount of coke produced [1, 4]. However, the reactions have not been confirmed by experiments, because the reactions are quite complex during pyrolysis and the temperature of pyrolysis is high to

650 °C. So this study aims to simulate the reactions by Gaussian09 based on density functional theory (DFT) to study its reaction mechanism and clarify the pyrolysis mechanism of cellulose and PE under the catalytic action of HZSM-5.

According to the results of Py-GC/MS experiments, the main products of cellulose pyrolysis are levoglucosan (LG) and acetol. Yayun Zhang et al. have studied the pyrolysis mechanism of cellulose in detail [35], so the calculation and simulation analysis were carried out directly from the reaction of cellulose pyrolysis product: acetol, furan, and its derivatives with vinyl and ethylene produced by pyrolysis cleavage isomerization of polyethylene.

The structure of furan and its derivatives produced by pyrolysis of cellulose and ethylene was optimized. After the optimization of the structure in Fig. 6 and the bond length of furan and ethylene in Table 3, the transition state of the two reactants was searched to obtain a transition state with one and only one imaginary frequency as shown in Fig. 7, and the optimization of the product is shown in Fig. 8. The bond length of transition state and product is given in Table 4. According to the transition state, it can be shown that in the reaction, the C1=C2 and C3=C4 in the furan ring are broken into a single bond, and the C–C undergoes an addition reaction with the ethylene double bond. The IRC calculation was performed on the transition state found. When the IRC was taken, the reactants and the product direction were simultaneously performed. As shown in Fig. 6, the results in the direction of the reactants were furan and ethylene, and the results in the product direction are shown in Fig. 8. After dehydration, aromatization, benzene, toluene, and the like are obtained.

Small molecule products produced by cellulose, such as acetone alcohol, were calculated and simulated to react with ethylene on HZSM-5. According to the optimization of the product, acetone alcohol and ethanol aldehyde cannot react with ethylene. However, the vinyl produced by the pyrolysis of polyethylene can react with a hydroxyl group to form a vinyl alcohol, and the radical reaction can

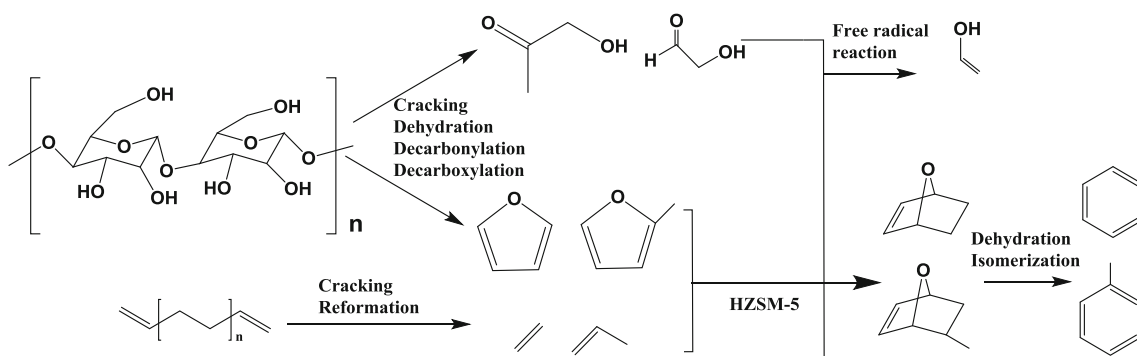
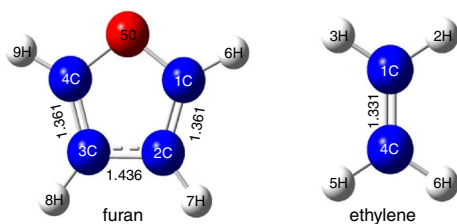


Fig. 5 Chemical mechanism of catalytic co-pyrolysis of cellulose and PE over HZSM-5



**Fig. 6** Optimization of furan and ethylene molecular

**Table 3** The bond length of furan and ethylene

Furan Parameters	Values Bond length Å	Ethylene Parameters	Values Bond length Å
C(4)-H(9)	1.079	C(4)-H(6)	1.088
C(4)-O(5)	1.364	C(4)-H(5)	1.088
C(3)-H(8)	1.081	C(1)-C(4)	1.331
C(3)-C(4)	1.361	C(1)-H(3)	1.088
C(2)-H(7)	1.081	C(1)-H(2)	1.088
C(2)-C(3)	1.436		
C(1)-H(6)	1.079		
C(1)-O(5)	1.364		
C(1)-C(2)	1.361		

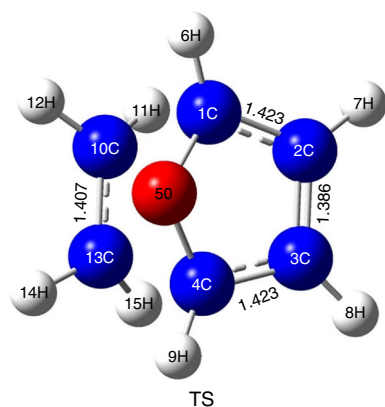


**Fig. 7** Transition state of the two reactants during co-pyrolysis reaction

release a lot of heat. Therefore, we initially included that the hydroxyl in the radical reaction came from the small molecular alcohols produced by cellulose pyrolysis.

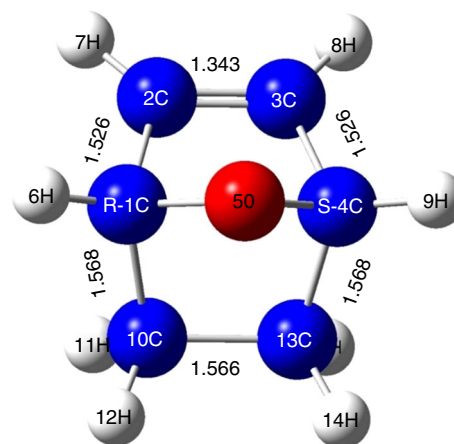


**Fig. 8** Optimization of the product in co-pyrolysis reaction

**Table 4** The bond length of transition state and Product

Transition state Parameters	Values Bond length Å	Product Parameters	Values Bond length Å
C(4)-H(17)	1.113	C(13)-H(15)	1.094
C(1)-H(16)	1.113	C(13)-H(14)	1.094
C(13)-H(15)	1.085	C(10)-C(13)	1.566
C(13)-H(14)	1.086	C(10)-H(12)	1.094
C(10)-C(13)	1.407	C(10)-H(11)	1.094
C(10)-H(12)	1.086	C(4)-C(13)	1.568
C(10)-H(11)	1.085	C(4)-H(9)	1.087
C(4)-H(9)	1.079	C(4)-O(5)	1.489
C(4)-O(5)	1.41	C(3)-H(8)	1.082
C(3)-H(8)	1.08	C(3)-C(4)	1.526
C(3)-C(4)	1.423	C(2)-H(7)	1.082
C(2)-H(7)	1.08	C(2)-C(3)	1.343
C(2)-C(3)	1.386	C(1)-C(10)	1.568
C(1)-H(6)	1.079	C(1)-H(6)	1.087
C(1)-O(5)	1.41	C(1)-O(5)	1.489
C(1)-C(2)	1.423	C(1)-C(2)	1.526

## Conclusions

This study showed that catalytic co-pyrolysis of cellulose and PE can improve the quality of produced bio-oil. The results of Py-GC/MS showed that the addition of PE and HZSM-5 greatly reduced the content of oxygenates in the pyrolysis products, and the proportion of oxygenates decreased from 92.8 to 28.3%. The kinds of products are decreased, and the content of ketones, esters, aromatic hydrocarbons, olefins, and alkanes is increased. The addition of HZSM-5 promotes the progress of the Diels–Alder reaction, so that the free radical reactions suppressed. Herein, the content of the alcohol compound is reduced.

The optimization and IRC calculation results show that the theoretical reaction process of catalytic co-pyrolysis is consistent with the proposed reaction process. The Diels–Alder reaction and the free radical reaction can be confirmed by optimization and IRC calculation. The reactions mechanism of catalytic co-pyrolysis of cellulose and PE was studied more precisely by the combination of DFT calculations and experiments.

**Acknowledgements** The authors are grateful for the financial supports from the Beijing Forestry University hot spot tracking project (No. 200-121701284), National Natural Science Foundation of China (Nos. 21838006, 21576155 and 21776159), and Research Project of Guangdong Provincial Department of Science and Technology Department (No. 2015B020215004).

## References

- Xue J, Zhuo J, Liu M, Chi Y, Zhang D, Yao Q. Synergetic effect of co-pyrolysis of cellulose and polypropylene over an all-silica mesoporous catalyst MCM-41 using thermogravimetry-fourier transform infrared spectroscopy and pyrolysis-gas chromatography-mass spectrometry. *Energy Fuels*. 2017;31(9):9576–84. <https://doi.org/10.1021/acs.energyfuels.7b01651>.
- Yang J, Rizkiana J, Widayatno WB, Karnjanakom S, Kaewpanha M, Hao X, et al. Fast co-pyrolysis of low density polyethylene and biomass residue for oil production. *Energy Convers Manag*. 2016;120:422–9. <https://doi.org/10.1016/j.enconman.2016.05.008>.
- Xue Y, Kelkar A, Bai X. Catalytic co-pyrolysis of biomass and polyethylene in a tandem micropyrolyzer. *Fuel*. 2016;166:227–36. <https://doi.org/10.1016/j.fuel.2015.10.125>.
- Li X, Li J, Zhou G, Feng Y, Wang Y, Yu G, et al. Enhancing the production of renewable petrochemicals by co-feeding of biomass with plastics in catalytic fast pyrolysis with ZSM-5 zeolites. *Appl Catal A*. 2014;481:173–82. <https://doi.org/10.1016/j.apcata.2014.05.015>.
- Brebu M, Ucar S, Vasile C, Yanik J. Co-pyrolysis of pine cone with synthetic polymers. *Fuel*. 2010;89(8):1911–8. <https://doi.org/10.1016/j.fuel.2010.01.029>.
- Li J, Li X, Zhou G, Wang W, Wang C, Komarneni S, et al. Catalytic fast pyrolysis of biomass with mesoporous ZSM-5 zeolites prepared by desilication with NaOH solutions. *Appl Catal A*. 2014;470:115–22. <https://doi.org/10.1016/j.apcata.2013.10.040>.
- Liu C, Wang H, Karim AM, Sun J, Wang Y. Catalytic fast pyrolysis of lignocellulosic biomass. *Chem Soc Rev*. 2014;43(22):7594–623. <https://doi.org/10.1039/c3cs60414d>.
- Dorado C, Mullen CA, Boateng AA. H-ZSM5 catalyzed co-pyrolysis of biomass and plastics. *ACS Sustain Chem Eng*. 2013;2(2):301–11. <https://doi.org/10.1021/sc400354g>.
- Zhang B, Zhong Z, Li T, Xue Z, Wang X, Ruan R. Biofuel production from distillers dried grains with solubles (DDGS) co-fed with waste agricultural plastic mulching films via microwave-assisted catalytic fast pyrolysis using microwave absorbent and hierarchical ZSM-5/MCM-41 catalyst. *J Anal Appl Pyrol*. 2018;130:1–7. <https://doi.org/10.1016/j.jaap.2018.02.007>.
- Xiang Z, Liang J, Morgan HM Jr, Liu Y, Mao H, Bu Q. Thermal behavior and kinetic study for co-pyrolysis of lignocellulosic biomass with polyethylene over cobalt modified ZSM-5 catalyst by thermogravimetric analysis. *Bioresour Technol*. 2018;247:804–11. <https://doi.org/10.1016/j.biortech.2017.09.178>.
- Ding K, He A, Zhong D, Fan L, Liu S, Wang Y, et al. Improving hydrocarbon yield via catalytic fast co-pyrolysis of biomass and plastic over ceria and HZSM-5: an analytical pyrolyzer analysis. *Bioresour Technol*. 2018;268:1–8. <https://doi.org/10.1016/j.biortech.2018.07.108>.
- Arregi A, Amutio M, Lopez G, Artetxe M, Alvarez J, Bilbao J, et al. Hydrogen-rich gas production by continuous pyrolysis and in-line catalytic reforming of pine wood waste and HDPE mixtures. *Energy Convers Manag*. 2017;136:192–201. <https://doi.org/10.1016/j.enconman.2017.01.008>.
- Zhang M, Geng Z, Yu Y. Density functional theory (DFT) study on the pyrolysis of cellulose: the pyran ring breaking mechanism. *Comput Theor Chem*. 2015;1067:13–23. <https://doi.org/10.1016/j.comptc.2015.05.001>.
- Chattopadhyay J, Pathak TS, Srivastava R, Singh AC. Catalytic co-pyrolysis of paper biomass and plastic mixtures (HDPE (high density polyethylene), PP (polypropylene) and PET (polyethylene terephthalate)) and product analysis. *Energy*. 2016;103:513–21. <https://doi.org/10.1016/j.energy.2016.03.015>.
- Chen T, Wu J, Zhang J, Wu J, Sun L. Gasification kinetic analysis of the three pseudocomponents of biomass-cellulose, semicellulose and lignin. *Bioresour Technol*. 2014;153:223–9. <https://doi.org/10.1016/j.biortech.2013.12.021>.
- Paradela F, Pinto F, Gulyurtlu I, Cabrita I, Lapa N. Study of the co-pyrolysis of biomass and plastic wastes. *Clean Technol Environ Policy*. 2008;11(1):115–22. <https://doi.org/10.1007/s10098-008-0176-1>.
- Chi Y, Xue J, Zhuo J, Zhang D, Liu M, Yao Q. Catalytic co-pyrolysis of cellulose and polypropylene over all-silica mesoporous catalyst MCM-41 and Al-MCM-41. *Sci Total Environ*. 2018;633:1105–13. <https://doi.org/10.1016/j.scitotenv.2018.03.239>.
- Wang S, Zhou Y, Liang T, Guo X. Catalytic pyrolysis of mannose as a model compound of hemicellulose over zeolites. *Biomass Bioenerg*. 2013;57:106–12. <https://doi.org/10.1016/j.biombioe.2013.08.003>.
- Li J, Yu Y, Li X, Wang W, Yu G, Deng S, et al. Maximizing carbon efficiency of petrochemical production from catalytic co-pyrolysis of biomass and plastics using gallium-containing MFI zeolites. *Appl Catal B*. 2015;172–173:154–64. <https://doi.org/10.1016/j.apcatb.2015.02.015>.
- Zhang X, Lei H, Zhu L, Zhu X, Qian M, Yadavalli G, et al. Thermal behavior and kinetic study for catalytic co-pyrolysis of biomass with plastics. *Bioresour Technol*. 2016;220:233–8. <https://doi.org/10.1016/j.biortech.2016.08.068>.
- Xue Y, Bai X. Synergistic enhancement of product quality through fast co-pyrolysis of acid pretreated biomass and waste plastic. *Energy Convers Manag*. 2018;164:629–38. <https://doi.org/10.1016/j.enconman.2018.03.036>.
- Kumagai S, Fujita K, Kameda T, Yoshioka T. Interactions of beech wood–polyethylene mixtures during co-pyrolysis. *J Anal Appl Pyrol*. 2016;122:531–40. <https://doi.org/10.1016/j.jaap.2016.08.012>.
- Hassan H, Lim JK, Hameed BH. Recent progress on biomass co-pyrolysis conversion into high-quality bio-oil. *Bioresour Technol*. 2016;221:645–55. <https://doi.org/10.1016/j.biortech.2016.09.026>.
- Gunasee SD, Danon B, Görgens JF, Mohee R. Co-pyrolysis of LDPE and cellulose: synergies during devolatilization and condensation. *J Anal Appl Pyrol*. 2017;126:307–14. <https://doi.org/10.1016/j.jaap.2017.05.016>.
- Cheng Y-T, Huber GW. Production of targeted aromatics by using Diels–Alder classes of reactions with furans and olefins over ZSM-5. *Green Chem*. 2012. <https://doi.org/10.1039/c2gc35767d>.
- Carlson TR, Jae J, Lin Y-C, Tompsett GA, Huber GW. Catalytic fast pyrolysis of glucose with HZSM-5: the combined



- homogeneous and heterogeneous reactions. *J Catal.* 2010;270(1):110–24. <https://doi.org/10.1016/j.jcat.2009.12.013>.
27. Al-Salem SM, Antelava A, Constantinou A, Manos G, Dutta A. A review on thermal and catalytic pyrolysis of plastic solid waste (PSW). *J Environ Manage.* 2017;197:177–98. <https://doi.org/10.1016/j.jenvman.2017.03.084>.
  28. Abnisa F, Wan Daud WMA, Ramalingam S, Azemi MNBM, Sahu JN. Co-pyrolysis of palm shell and polystyrene waste mixtures to synthesis liquid fuel. *Fuel.* 2013;108:311–8. <https://doi.org/10.1016/j.fuel.2013.02.013>.
  29. Abnisa F, Wan Daud WMA. A review on co-pyrolysis of biomass: an optional technique to obtain a high-grade pyrolysis oil. *Energy Convers Manag.* 2014;87:71–85. <https://doi.org/10.1016/j.enconman.2014.07.007>.
  30. Wang S, Guo X, Liang T, Zhou Y, Luo Z. Mechanism research on cellulose pyrolysis by Py-GC/MS and subsequent density functional theory studies. *Bioresour Technol.* 2012;104:722–8. <https://doi.org/10.1016/j.biortech.2011.10.078>.
  31. Zhang M, Geng Z, Yu Y. Density functional theory (DFT) study on the dehydration of cellulose. *Energy Fuels.* 2011;25(6):2664–70. <https://doi.org/10.1021/ef101619e>.
  32. Zhang Y, Liu C, Chen X. Unveiling the initial pyrolytic mechanisms of cellulose by DFT study. *J Anal Appl Pyrol.* 2015;113:621–9. <https://doi.org/10.1016/j.jaap.2015.04.010>.
  33. Zhang J, Chen T, Wu J, Wu J. Multi-gaussian-DAEM-reaction model for thermal decompositions of cellulose, hemicellulose and lignin: comparison of N(2) and CO(2) atmosphere. *Bioresour Technol.* 2014;166:87–95. <https://doi.org/10.1016/j.biortech.2014.05.030>.
  34. Mihalcik DJ, Mullen CA, Boateng AA. Screening acidic zeolites for catalytic fast pyrolysis of biomass and its components. *J Anal Appl Pyrol.* 2011;92(1):224–32. <https://doi.org/10.1016/j.jaap.2011.06.001>.
  35. Lorenzetti C, Conti R, Fabbri D, Yanik J. A comparative study on the catalytic effect of H-ZSM5 on upgrading of pyrolysis vapors derived from lignocellulosic and proteinaceous biomass. *Fuel.* 2016;166:446–52. <https://doi.org/10.1016/j.fuel.2015.10.051>.
  36. Cepeliogullar O, Putun AE. A pyrolysis study for the thermal and kinetic characteristics of an agricultural waste with two different plastic wastes. *Waste Manag Res.* 2014;32(10):971–9. <https://doi.org/10.1177/0734242X14542684>.
  37. Kim Y-M, Lee HW, Jae J, Jung KB, Jung S-C, Watanabe A, et al. Catalytic co-pyrolysis of biomass carbohydrates with LLDPE over Al-SBA-15 and mesoporous ZSM-5. *Catal Today.* 2017;298:46–52. <https://doi.org/10.1016/j.cattod.2017.06.006>.
  38. Karimi E, Teixeira IF, Gomez A, de Resende E, Gissane C, Leitch J, et al. Synergistic co-processing of an acidic hardwood derived pyrolysis bio-oil with alkaline red mud bauxite mining waste as a sacrificial upgrading catalyst. *Appl Catal B.* 2014;145:187–96. <https://doi.org/10.1016/j.apcatb.2013.02.007>.
  39. Zhang H, Xiao R, Nie J, Jin B, Shao S, Xiao G. Catalytic pyrolysis of black-liquor lignin by co-feeding with different plastics in a fluidized bed reactor. *Bioresour Technol.* 2015;192:68–74. <https://doi.org/10.1016/j.biortech.2015.05.040>.
  40. Sajdak M. Impact of plastic blends on the product yield from co-pyrolysis of lignin-rich materials. *J Anal Appl Pyrol.* 2017;124:415–25. <https://doi.org/10.1016/j.jaap.2017.03.002>.
  41. Liu M, Yang J, Liu Z, He W, Liu Q, Li Y, et al. Cleavage of covalent bonds in the pyrolysis of lignin, cellulose, and hemicellulose. *Energy Fuels.* 2015;29(9):5773–80. <https://doi.org/10.1021/acs.energyfuels.5b00983>.
  42. Sajdak M, Muzyka R, Hrabak J, Słowik K. Use of plastic waste as a fuel in the co-pyrolysis of biomass. *J Anal Appl Pyrol.* 2015;112:298–305. <https://doi.org/10.1016/j.jaap.2015.01.008>.
  43. Ru B, Wang S, Dai G, Zhang L. Effect of torrefaction on biomass physicochemical characteristics and the resulting pyrolysis behavior. *Energy Fuels.* 2015;29(9):5865–74. <https://doi.org/10.1021/acs.energyfuels.5b01263>.
  44. Wang S, Ru B, Dai G, Sun W, Qiu K, Zhou J. Pyrolysis mechanism study of minimally damaged hemicellulose polymers isolated from agricultural waste straw samples. *Bioresour Technol.* 2015;190:211–8. <https://doi.org/10.1016/j.biortech.2015.04.098>.
  45. Zhao C, Jiang E, Chen A. Volatile production from pyrolysis of cellulose, hemicellulose and lignin. *J Energy Inst.* 2017;90(6):902–13. <https://doi.org/10.1016/j.joei.2016.08.004>.
  46. Yang X, Zhao Y, Li R, Wu Y, Yang M. A modified kinetic analysis method of cellulose pyrolysis based on TG–FTIR technique. *Thermochim Acta.* 2018;665:20–7. <https://doi.org/10.1016/j.tca.2018.05.008>.

**Publisher's Note** Springer Nature remains neutral with regard to jurisdictional claims in published maps and institutional affiliations.